Measurement of the convective moisture transfer coefficient from porous building material surfaces applying a wind tunnel method

Goce Talev[a,b,*], Bjørn Petter Jelle[a,b], Erling Næss[c], Arild Gustavsen[d] and Jan Vincent Thue[a]

[a] Department of Civil and Transport Engineering, Norwegian University of Science and Technology (NTNU), Trondheim, Norway.

[b] Department of Materials and Structures, SINTEF Building and Infrastructure, Trondheim, Norway.

[c] Department of Energy and Process Engineering, Norwegian University of Science and Technology (NTNU), Trondheim, Norway.

[d] Department of Architectural Design, History and Technology, Norwegian University of Science and Technology (NTNU), Trondheim, Norway.

* Corresponding author: goce.talev@reinertsen.com

ABSTRACT: This paper presents results for the average convective moisture transfer coefficients (CMTC) of several porous building material samples exposed to air-flow. The experimental measurements explore the effect of the various air velocities, temperatures and local positions on the average convective moisture transfer coefficients. Selected building materials were soaked in distilled water at least two weeks before the measurements. A thin building specimen with moisture content close to the saturation point was mounted in level with the bottom wind tunnel surface. A stable airflow regime was measured over the thin samples placed in the specimen holder. Water from the sample holder was absorbed from the bottom side of the building materials and evaporated from the upper side of the specimen during the airflow exposure. Two different membranes were fixed over the water cup as reference materials for comparison. The measurements were carried out at (50 ± 3) % relative humidity, air temperatures 23.6 ± 0.5°C, 26.5 ± 0.5°C and 30.0 ± 0.5°C, and air velocities 1.1 m/s, 3.0 m/s and 5.5 m/s. The experimental data show that the convective moisture transfer coefficient is a function of velocity, temperature difference between the ambient air and material surface, local position as well as of the material type. The experimental results from water surfaces were compared to expressions for the convective moisture transfer coefficients from the literature.

1 INTRODUCTION

The moisture balance in indoor space can be strongly influenced by the moisture buffering of the room surfaces and furnishings, the ventilation rate, possible condensation on cold surfaces, moisture sources, the variation of these parameters with time and finally the outdoor weather conditions. Most building materials are porous and through absorption and desorption they have the ability to attenuate the moisture variation of the indoor air. Efficient ventilation and climate control of the indoor space may accelerate the moisture transfer process across the material surfaces. Consequently, moderation of the indoor relative humidity variation requires considerable practical experience and theoretical knowledge of the convective moisture transfer coefficients. This can be aided by the use of predictive design tools such as simulation software that can accurately model heat and moisture transport (Grausse et al., 1985). The convective moisture transfer coefficient and fundamental material properties such as input values to the numerical software play an important role to accurately estimate the

moisture exchange mechanisms through a material surface. Moisture buffering describes the ability of the building materials to moderate the relative humidity level in the indoor climate. Through absorption and desorption building materials with the ability to absorb and release moisture can be used to buffer the relative humidity level in the indoor climate.

Evaporation from free water or saturated surfaces has received some attention from researchers with regard to determination of evaporation rate. Several studies of the convective moisture (or mass) transfer coefficient (CMTC) for water or saturated non-wood surfaces as a function of air velocity (free stream velocity u_∞) have been published, e.g. Carrier (1921), Hinchley and Himus (1924). For further information it is referred to the literature, e.g. the studies by Lurie and Michailoff (1936), Jason (1958), Wadsö (1993), Jacobsen and Aarseth (1999), Derome (2004), Iskra and Simonson (2005), and the brief summary by Talev et al. (2008a). The use of the hygroscopic building materials to improve the indoor humidity conditions has been a hygrothermal research topic in the last 20 years. Today there is increased interest which includes the analyses of the moisture buffering properties. Thus, based on the above discussion there is a need for research on the buffering effects of materials used in buildings, and the boundary conditions, in order to predict the indoor temperature and relative humidity by numerical simulations.

A new open-loop, low-speed wind tunnel with an unique design has been constructed at the Norwegian University of Science and Technology (NTNU), intended to allow testing of different building materials under a wide range of flow conditions (Talev et al. 2008b). The primary goal of the wind tunnel design was to provide experimental information about the convective moisture transfer coefficient as a function of the exterior boundary conditions and material properties of various specimens. In order to carry out the desired measurements, the wind tunnel should meet the following two requirements:

a) The velocity profile through the test section should be as near as possible to a parallel steady flow with uniform speed (straightened), with relevant boundary layer thickness along the surface,

b) Turbulence intensity should be as close as possible to zero to facilitate the comparison of results, and to avoid velocity fluctuations within the wind tunnel.

The knowledge of the influence of the free stream air velocity (u_∞) across a moist surface in combination with the effects of concentration (δ_c) and thermal (δ_t) boundary layers on the moisture transfer rate is essential in order to describe and predict the moisture interactions between the construction and the ambient air. Therefore, the experiments in this work focuses on the determination of the average convective moisture transfer coefficients (β) from several saturated materials as a function of the free stream air velocity (u_∞). The relative humidity of the air (φ) was (50 ± 3) % and the unheated and no-evaporation starting length (ξ) was constant during the experiments.

2 THEORY

2.1 General

Determination of the convective moisture transport through a given boundary layer with an unheated and no mass transfer starting length, upstream the water pool, have been a challenge for many researchers. The solutions of the external airflow over a flat plate where the moisture transfer (evaporation) starts at point $x = \xi$ on the plate, rather than at $x = 0$, where the

velocity boundary layer starts, are based on fundamental boundary layer theory. A velocity boundary layer is assumed thicker than the concentration boundary layer thickness ($\delta_u > \delta_c$) is shown in Figure 1.

Laminar air flow analysis along a flat plate, including a starting length ξ with no mass transfer results, by analogy with heat transfer, in the local Sherwood number Sh_x as a function of the local position x, Schmidt number Sc and local Reynolds number Re_x, (Kays and Crawford, 1993):

$$Sh_x = \frac{0.332 \cdot Sc^{\frac{1}{3}} \cdot \sqrt{\mathrm{Re}_x}}{\left[1 - \left(\frac{\xi}{x}\right)^{\frac{3}{4}}\right]^{\frac{1}{3}}} \quad \text{, where } x > \xi \tag{1}$$

The Schmidt number is a physical properties group relating the fluid kinematic viscosity to the mass (moisture) diffusivity, i.e

$$Sc = \frac{\nu}{D_{AB}} \tag{2}$$

Here, ν is the fluid kinematic viscosity and D_{AB} is the binary mass diffusivity of component A in a fluid B.

The local Reynolds number (Re_x) represents a flow regime. Also, the local Reynolds number Re_x may be interpreted as a ratio of the fluid inertia forces (destabilizing forces) to the stabilizing forces (viscosity).

$$\mathrm{Re}_x = \frac{\rho \cdot u_\infty \cdot x}{\mu} = \frac{u_\infty \cdot x}{\nu} \tag{3}$$

External laminar flow is found for Re_x less than approximately $3 \cdot 10^5$ (Incropera and deWitt 2002).

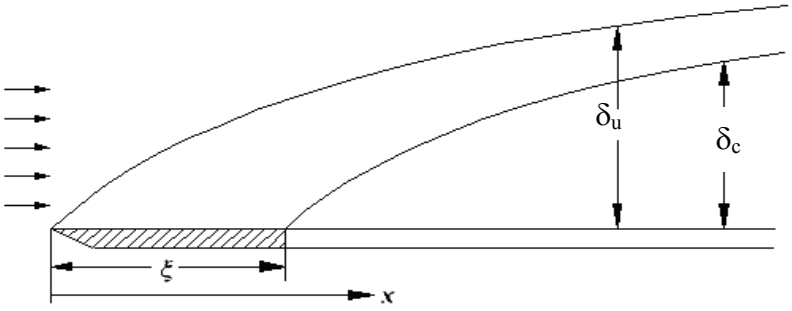

Figure 1. Boundary layer development on a flat plate with unheated and no-evaporation starting length. δ_u represents the velocity (momentum) boundary layer (m) while δ_c is concentration boundary layer thickness (m).

From an analysis of turbulent external flow the corresponding expression may be written as (Kays and Crawford, 1993):

$$Sh_x = \frac{0.0287 \cdot \mathrm{Re}_x^{0.8} \cdot Sc^{0.6}}{\left[1 - \left(\frac{\xi}{x}\right)^{0.9}\right]^{\frac{1}{9}}} \quad \text{, where } x > \xi \tag{4}$$

Where there is not evaporation for $0 < x < \xi$ and $L > \xi$. The local convective mass transfer coefficients are readily determined from Eq.1 and Eq. 4, using the definition of Sh_x given as

$$Sh_x = \frac{\beta_x \cdot x}{D_{AB}} \tag{5}$$

where β_x is the local convective mass transfer coefficient and D_{AB} is the mass diffusivity.

The average moisture transfer coefficients obtained by integrating the local expressions between x=0 and x=L, resulting in (Thomas, 1977):

Laminar: $$\overline{\beta_l} = \frac{2 \cdot [1 - \left(\frac{\xi}{L}\right)^{\frac{3}{4}}]}{1 - \frac{\xi}{L}} \beta_{x=L} \tag{6}$$

Turbulent: $$\overline{\beta_t} = \frac{5 \cdot [1 - \left(\frac{\xi}{L}\right)^{\frac{9}{10}}]}{4(1 - \frac{\xi}{L})} \beta_{x=L} \tag{7}$$

2.2 **Interpretation of experimental results**

The average convective moisture (or mass) transfer coefficient $\overline{\beta}$ was calculated from the following relationship

$$\overline{\beta_p} = \frac{m}{A\left(P_{v,s} - P_{v,\infty}\right)t} \qquad (\mathrm{kg/(m^2 \cdot Pa \cdot s)}) \tag{8}$$

In building physics, density difference is commonly identified as a driving potential for mass transfer. This is a reasonable approach for small temperature differences. Under such conditions, the convective moisture transfer coefficient may be expressed by

$$\overline{\beta} = \frac{m}{A\left(\rho_{v,s} - \rho_{v,\infty}\right)t} \qquad (\mathrm{m/s}) \tag{9}$$

where m (kg) is the mass of the evaporated water, A (m^2) is the exposed upper specimen area (towards the wind tunnel air flow), $\rho_s - \rho_\infty$ (kg/m^3) is the water vapour density difference between the surface and the free stream, and t (s) is the elapsed time.

The mass of evaporated water per area (*m/A*) from the sample holder during the evaporation process was determined from the scale readings of an additional container placed outside the wind tunnel.

The air at the water surface was assumed saturated, and thus the water vapour pressure at the water surface was based on the saturation pressure of water at the surface temperature. The water vapour and the air were treated as ideal gases. Total atmospheric pressure is a sum of vapour and dry air pressure. The density of the water vapour, dry air, and their mixture at the water-air interface and in the free stream are determined by (from ideal gas law):

At the water surface:

$$\rho_{v,s} = \frac{P_{v,s}}{R_v \cdot T_s}; \qquad \rho_{a,s} = \frac{P_{a,s}}{R_a \cdot T_s} \tag{10}$$

$$\rho_s = \rho_{v,s} + \rho_{a,s} \tag{11}$$

where $P_{v,s}$ is saturation pressure of water vapor interphase (Pa), R_v= 461.52 (J/(kg·K)) is the specific gas constant for water vapour, R_a= 287.06 (J/(kg·K)) represents the specific gas constant of dry air and T_s is the water-surface temperature.

At free stream conditions:

$$\rho_{v,\infty} = \frac{P_{v,\infty}}{R_v \cdot T_\infty}; \qquad \rho_{a,\infty} = \frac{P_{a,\infty}}{R_a \cdot T_\infty} \tag{12}$$

$$\rho_\infty = \rho_{v,\infty} + \rho_{a,\infty} \tag{13}$$

The water vapour pressure in the free stream (far from the water surface) was calculated from

$$P_{v,\infty} = \varphi \cdot P_{sat,T_\infty} \tag{14}$$

where the relative humidity of air is denoted as φ. In order to determine the convective moisture transfer coefficients with pressure as a driving force β_p (Eq.8), the saturated water vapour pressure at the water surface is calculated by

$$P_{v,s} = \rho_{v,s} \cdot R_v \cdot T_s \tag{15}$$

where the specific gas constant for water vapour R_v is the molar (universal) gas constant R = 8.314 (J/(mol·K)) divided by the molar mass of water vapour M = 18.02 g/mol. The derivation above follows from the ideal gas law PVT = nR, noting that the number of moles n = m/M and mass density ρ = m/V, give ρ = P/((R/M)T) = P/($R_{specific}$T).

3 EXPERIMENTAL

The experimental work was performed in a wind tunnel located in a climate room as shown in Figure 2. The design and construction of the wind tunnel are presented by Talev et al. (2008b)

and Talev et al. (2009). Thin specimens with a thickness of 11.7 ± 0.5 mm of Baumberger sandstone, Worzeldorfer sandstone, Sander sandstone, Krensheimer shelly limestone and gypsum board (with cardboard) were selected. All the material samples were soaked in distilled water before they were placed in the sample holder. The selected building material specimens with high moisture content (close to the saturation) were exposed at various air velocities, temperatures and local positions. All experiments were run with constant inlet relative air humidity of (50 ± 3) %. The material properties of selected materials are presented in Table 1.

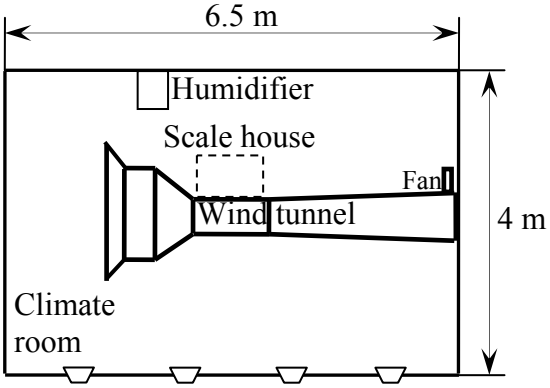

Figure 2. Position of the wind tunnel in the climate room.

Three equal water sample holders per line, with a total of three lines (i.e. a total of nine sample holders) were placed in the wind tunnel, see Figure 3. Measurements were performed on the middle sample holder of each line. Each sample holder had a quadratic shape with side lengths of 50 mm and the sample top surfaces were mounted in level with the bottom of the wind tunnel floor. The sample holders were manufactured from aluminium and were easily removable and adjustable from below the tunnel floor.

The bottom of the sample holder was connected to a water container through a pipe with high thermal conductivity. The water container had a diameter of 15 cm and was placed on a scale. The primary function of the water container was to supply the sample holder with water and keep the water surface in the sample holder at level with the wind tunnel floor (or any desired level). The desired water level in the sample holder was maintained by an additional glass pipe, having an initial diameter of 1.5 mm and a measuring scale that was attached on the side of the water container see Figure 4. The removed (evaporated) water from the sample holder was continuously replenished from the water container. The scale and the water container were placed in a specially designed scale house, see Figure 2. The primary function of the scale housing was to avoid undesired influence from the ambient room air flow to the scale. The amount of water transported from the water container to the sample holder was noted by the scale for each minute through an interface to a personal computer outside the climate room. The experiments showed that the water level in the container would decrease by 1 mm for each 17.6 g water evaporated. The maximum water evaporated was about 5 g at maximum air velocity air temperature, taking about four hours. Hence, it may be stated that this system provides a sufficiently constant water level in the sample holder.

Table 1. Material properties, dry materials (WUFI 4.2, Fraunhofer Institute (2006)).

Material	Bulk density (kg/m^3)	Porosity (m^3/m^3)	Heat capacity (J/(kgK))	Thermal conductivity (W/(mK))	Diffusion resistance factor μ (-)
Baumberger sandstone	1980	0.23	850	1.70	20
Worzeldorfer sandstone	2263	0.13	850	1.80	26
Sander sandstone	2120	0.13	850	1.60	33
Krensheimer shelly limestone	2440	0.13	850	2.25	140

Figure 3. Test section of the wind tunnel.

The water container lid was specially designed and mounted on the top of the water container. The primary function of the container lid holes was to provide the balance between the ambient and container air pressure. The edges of the water container lid were taped with aluminium tape to the body of the water container. The experimental work showed that a completely closed water container would cause very unstable air pressure over the water surface in the container, and lead to serious measurement errors. In order to improve the method, several holes with diameter 2 mm were made in the container lid. A metal pin was put in each hole, see Figure 4.

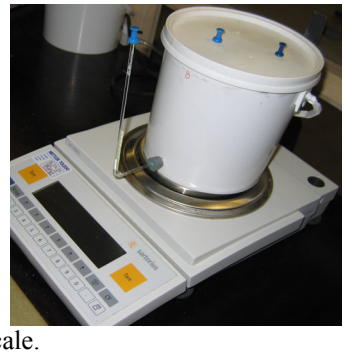

Figure 4. Water container placed on a scale.

A cylindrical copper table was placed in the middle of the sample holder as shown in Figure 5. The height of the cylindrical copper table was defined as the difference between the total depth of the sample holder and the material thickness. The primary function of the cylindrical table was to hold the samples flush with the bottom surface during the measurements. It was immersed in water during the experiment duration. The top area of the copper table was specially designed. It provides better water supply to the material sample as well as it reduced

the contact area between the material samples and the copper table. In order to avoid any undesired water supply problems several holes were made on the copper body as presented in Figure 5.

Figure 5. Cylindrical copper table.

The water surface temperature was measured using three thermocouples, and the average surface temperature was based on a minimum of three measurement for each air temperature and air velocity used. The average measured temperatures, together with the material properties of the air, were used for the calculation procedure given in the appendix.

The selected material was placed inside the sample holder just above the copper table. The side edges of each tested material specimen were insulated with silicon. It enabled water to be absorbed from only the bottom of the sample and thus achieve one-dimensional moisture transfer. All the material samples were soaked in distilled water before they were placed in the sample holder. A thin metal plate with thickness 0.4 mm an opening area of 35 mm x 35 mm (at the centre of the metal plate) was added above the material surface. The metal plate was used to avoid any additional moisture transfer which might occur between the sample holder walls and the edges of the building material. The other advantage of using the same metal plate was the fact that the constant moisture transfer area was provided for each experiment.

Various airflow velocities were provided by a suction fan mounted on the back side of the wind tunnel, see Figure 2. Average free-stream velocity at a position 150 mm upstrem the tested samples was measured using a pitot static tube attached to a probe traversing system and connected to a micro-manometer. The air velocity measurement uncertainties are presented in Tables 2, 3 and 4.

As part of the validation and to determine the zero level baselines for the system, a metal plate was also tested. The metal plate was flush with the wind tunnel floor. The lifting forces that exist inside the test section could influence the position of the metal place since it is very light. Three measurements periods of 4 hours for each sample holder at maximum air velocity were carried out. Measurements accuracy of ± 0.01 g was noted. In order to overcome the lift force as well as to avoid any diffusion from the water sample, the edges of the metal plate were taped to the bottom wall of the test section.

4 RESULTS AND DISCUSSION

4.1 Materials exposed at various air velocities

The results from the wind tunnel experiments, measured on in the middle cup of the second line, using various building materials are presented in Figure 6, Figure 7 and Figure 8 for air velocities of 1.1 m/s, 3.0 m/s and 5.5 m/s, respectively. The results are summarized in Table 2, which also includes calculated convective moisture transfer coefficients for the various materials and the three different wind tunnel velocities.

The graphs in Figures 6-8 depict the accumulated evaporated amount of water evaporated per unit exposed surface from the material surfaces with high moisture content (close to the saturation point) versus time for a period of 4 hours. As the accumulated evaporated mass per unit area is approximately linear, it means that the instant evaporation flux (mass per unit area and time) and the convective moisture transfer coefficient (from Eq.8 and Eq.9) are approximately constant for the entire measurement period of 4 hours. All the presented accumulated evaporation fluxes given in Figures 6-8 are calculated averages from minimum three measurement periods of 4 hours for each material and air velocity.

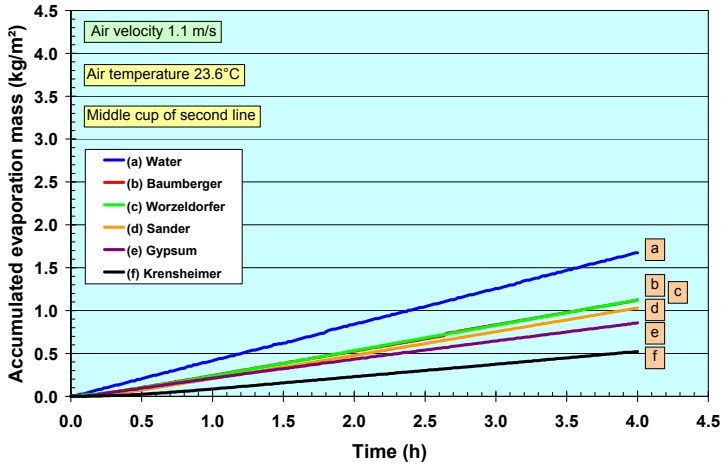

Figure 6. Accumulated evaporation mass vs. time for various materials at an air velocity of 1.1 m/s and air temperature of 23.6°C. Experiments were performed in the middle cup of the second line.

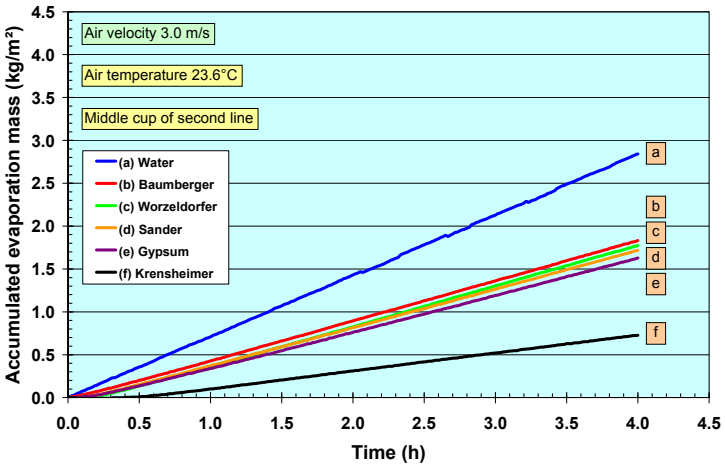

Figure 7. Accumulated evaporation mass vs. time for various materials at an air velocity of 3.0 m/s and air temperature of 23.6°C. Experiments were performed in the middle cup of the second line.

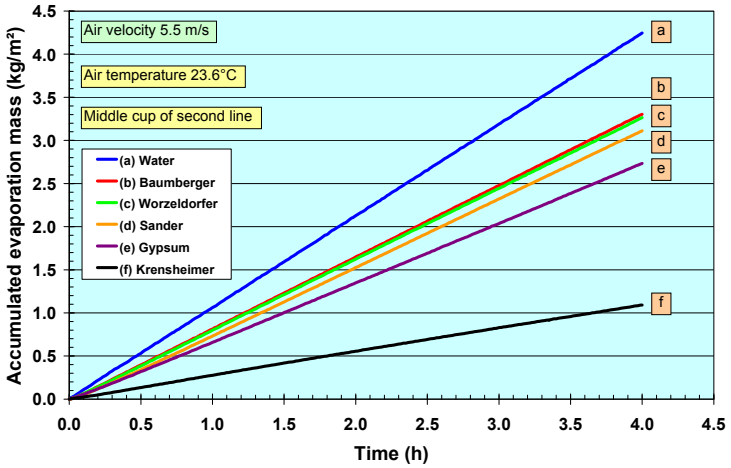

Figure 8. Accumulated evaporation mass vs. time for various materials at an air velocity of 5.5 m/s and air temperature of 23.6°C. Experiments were performed in the middle cup of the second line.

A high evaporation mass per unit area yields a high CMTC at constant temperature difference between the water surface and free stream, which should be noted in the following discussion below.

As expected for all materials it is observed that the mass evaporation (per area) is largest for the highest air velocity. It is also observed, still as expected, that the evaporation mass for water is higher than the mass evaporation for all other materials, i.e. higher evaporation flux from a water surface than from a porous material surface with high moisture content close to or being saturated (e.g. Worzeldorfer).

Water has the highest mass evaporation rate and thereby the highest apparent convective moisture transfer coefficient. Thereafter follow Baumberger sandstone, Worzeldorfer sandstone and Sander sandstone at almost the same level within the uncertainty limits. A bit lower than these follows the gypsum board, which in fact is considerably lower at the lowest wind velocity. At last, the lowest mass evaporation is found for the Krensheimer limestone. It has been noted that the material with the lowest diffusion resistance factor μ (Baumberger sandstone) has the highest mass evaporation, while the material with the highest diffusion resistance factor μ, Krensheimer limestone, has the lowest mass evaporation.

Theoretical values for the average convective moisture transfer coefficients for water, calculated by Eq.8 at 1.1 m/s at an air temperature of 23.6°C were $(10.559)\cdot10^{-3}$ m/s for the laminar case (Eq.6). The experimental result from Table 2 is $(11.10 \pm 0.19)\cdot10^{-3}$ m/s. In addition, the theoretical convective moisture transfer coefficient for water surface at 3.0 m/s and 5.5 m/s were calculated to be $(18.091)\cdot10^{-3}$ m/s and $(24.302)\cdot10^{-3}$ m/s, respectively. Again the experimental results from Table 2 are $(18.5 \pm 0.2)\cdot10^{-3}$ and $(26.81 \pm 0.16)\cdot10^{-3}$ m/s. The velocity profile in an empty wind tunnel according to Reynolds number for external flow (see Eq.3) was found to be laminar even though the boundary layer thickness has not been measured.

Table 2. Convective moisture transfer coefficient β and evaporation mass for various materials at three wind velocities. Air temperature is about 23.6°C. Middle cup of second line. See Figures 6-8.

Material	*Air velocity* (m/s)	*Mass change* (g)	*Evaporation mass* (kg/m^2)	$\overline{\beta}_p$ (10^{-9} $kg/(m^2 \cdot Pa \cdot s)$)	$\overline{\beta}$ (10^{-3} m/s)
Water	1.07 ± 0.04	2.05 ± 0.02	1.67 ± 0.01	77.8 ± 0.7	11.10 ± 0.19
	3.05 ± 0.04	3.48 ± 0.04	2.84 ±0.03	132.1 ± 1.4	18.5 ± 0.2
	5.53 ± 0.12	5.20 ± 0.03	4.25 ±0.03	197.2 ± 1.2	26.81 ± 0.16
Baumberger sandstone	1.08 ± 0.06	1.38 ± 0.02	1.13 ± 0.01	52.4 ± 0.7	7.45 ± 0.09
	3.03 ± 0.03	2.24 ± 0.05	1.83 ± 0.06	84.9 ± 0.3	11.9 ± 0.4
	5.49 ± 0.12	4.1 ± 0.3	3.3 ± 0.2	153 ± 11	20.9 ± 1.5
Worzeldorfer sandstone	1.14 ± 0.10	1.38 ± 0.05	1.13 ± 0.04	52 ± 2	7.4 ± 0.3
	3.01 ± 0.04	2.17 ± 0.03	1.77 ± 0.02	82.4 ± 1.0	11.51 ± 0.14
	5.51 ± 0.41	4.00 ± 0.13	3.27 ± 0.11	152 ± 5	20.6 ± 0.7
Sander sandstone	1.08 ± 0.05	1.26 ± 0.08	1.03 ± 0.07	48 ± 3	6.8 ± 0.5
	2.99 ± 0.04	2.11 ± 0.07	1.72 ± 0.06	80 ± 3	11.2 ± 0.4
	5.51 ± 0.03	3.81 ± 0.05	3.11 ± 0.04	144.5 ± 1.8	19.6 ± 0.2
Gypsum board	1.07 ± 0.04	1.05 ± 0.04	0.86 ± 0.03	39.8 ± 1.3	5.67 ± 0.19
	3.01 ± 0.04	1.99 ± 0.06	1.63 ± 0.05	75.4 ± 1.9	10.6 ± 0.3
	5.51 ± 0.13	3.4 ± 0.4	2.7 ± 0.4	127 ± 16	17.3 ± 2
Krensheimer limestone	1.09 ± 0.04	0.64 ± 0.04	0.52 ± 0.03	24.2 ± 1.5	3.4 ± 0.2
	3.01 ± 0.03	0.89 ± 0.04	0.73 ± 0.03	33.7 ± 1.3	4.72 ± 0.18
	5.43 ± 0.04	1.34 ± 0.19	1.10 ± 0.14	52 ± 6	6.9 ± 0.9

Uncertainty levels are given as the standard deviation of the mean with a 99.73 % confidence interval.

From Table 2 it is found that the experimental method is able to measure the convective moisture transfer coefficient and distinguish between various materials within acceptable uncertainty levels.

4.2 **Materials exposed at various air temperatures**

The results from the wind tunnel experiments, performed in the middle cup of the second line, with the building material Baumberger sandstone (and water as a reference) at three different temperatures, are presented in Figure 9 for an air velocity of about 3.0 m/s. The average measured values of the convective moisture transfer coefficients and their corresponding uncertainties are presented in Table 3.

Figure 9 shows the accumulated evaporated amount of water per exposed area from water surface and Baumberger sandstone for a time period of 4 hours. The accumulated mass evaporation mass per unit area is approximately linear, including that the convective moisture transfer coefficient (Eq.8 and Eq.9) is approximately constant for the entire measurement duration of 4 hours.

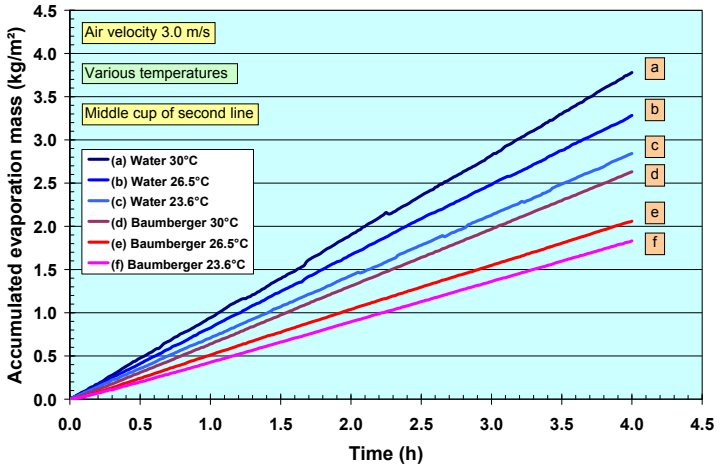

Figure 9. Accumulated evaporation mass vs. time for various temperatures at an air velocity of 3.0 m/s. Experiments were performed in the middle cup of the second line.

Table 3. Convective moisture transfer coefficient β and evaporation mass for Baumberger sandstone and water surface at three temperatures. Air velocity is about 3.0 m/s. Middle cup of second line. See Figure 9.

Material	*Air Velocity* (m/s)	*Air Temperature* (°C)	*Mass change* (g)	*Evaporation Mass* (kg/m^2)	$\overline{\beta}_p$ (10^{-9} $kg/(m^2 \cdot Pa \cdot s)$)	$\overline{\beta}$ (10^{-3} m/s)
Water	3.05 ± 0.04	23.6 ± 0.9	3.48 ± 0.04	2.84 ±0.03	132.1 ± 1.4	18.5 ± 0.2
	3.07 ± 0.02	26.5 ± 0.9	4.02 ± 0.15	3.28 ± 0.12	154 ± 6	21.8 ± 0.8
	2.99 ± 0.06	30.0 ± 0.9	4.63 ± 0.10	3.78 ± 0.08	179 ± 4	24.6 ± 0.5
Baumberger sandstone	3.03 ± 0.04	23.6 ± 0.9	2.24 ± 0.05	1.83 ± 0.06	84.9 ± 0.3	11.9 ± 0.4
	3.06 ± 0.02	26.5 ± 0.9	2.52 ± 0.04	2.06 ± 0.03	96.5 ± 1.3	13.7 ± 0.2
	2.98 ± 0.04	30.0 ± 0.9	2.75 ± 0.04	2.25 ± 0.03	106.5 ± 1.4	14.60± 0.15

Uncertainty levels are given as the standard deviation of the mean with a 99.7 % confidence interval.

It was noted that increasing the air temperature increased the temperature difference between the water surface and free stream air, leading to higher mass evaporation. In addition, the concentration difference, expressed by density, between the water surface and free stream air showed almost constant value of the concentration difference. This can explain the fact that increasing the air temperature leads to higher convective moisture transfer coefficient.

4.3 **Materials exposed at various local positions**

The results from the wind tunnel experiments, performed at various local positions, with the building material Baumberger sandstone (and water as a reference) at an air temperature of 30°C, are presented in Figure 10 for an air velocity of about 3.0 m/s. The average measured values of the convective moisture transfer coefficients and their corresponding uncertainties are presented in Table 4. Again the accumulated mass evaporation per unit area is approximately linear, that means the convective moisture transfer coefficient (from Eq.8 and Eq.9) is approximately constant for the measurement period of 4 hours.

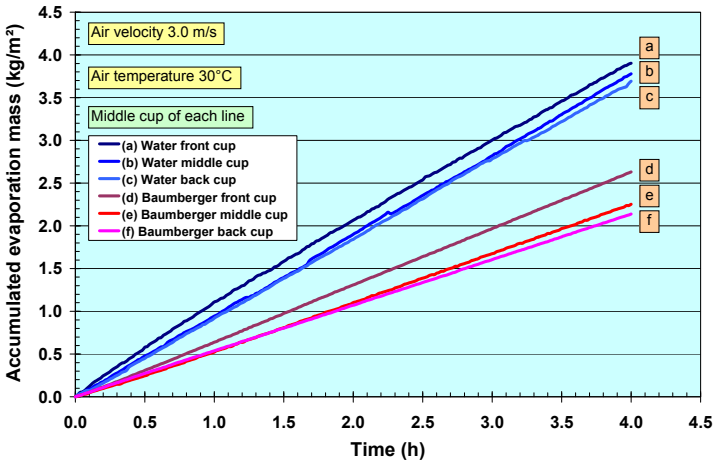

Figure 10. Accumulated evaporation mass vs. time for various local positions at an air velocity of 3.0 m/s and air temperature of 30°C.

Table 4. Convective moisture transfer coefficient β and evaporation mass for Baumberger and water surface at three various local positions. Air velocity is about 3.0 m/s while air temperature is about 30°C. See Figure 10.

Material	*Air velocity* (m/s)	*Local position*	*Mass change* (g)	*Evaporation mass* (kg/m^2)	$\overline{\beta}_p$ (10^{-9} kg/(m^2·Pa·s))	$\overline{\beta}$ (10^{-3} m/s)
Water	3.00 ± 0.08	Front cup	4.80 ± 0.05	3.92 ± 0.06	186 ± 3	25.5 ± 0.4
	2.99 ± 0.06	Middle cup	4.63 ± 0.10	3.78 ± 0.08	179 ± 4	24.6 ± 0.5
	2.96 ± 0.08	Back cup	4.52 ± 0.04	3.69 ± 0.03	174.9 ± 1.3	23.95 ± 0.18
Baumberger sandstone	3.01 ± 0.09	Front cup	3.22 ± 0.11	2.63 ± 0.09	124 ± 4	17.1 ± 0.6
	2.98 ± 0.04	Middle cup	2.75 ± 0.04	2.25 ± 0.03	106.5 ± 1.4	14.60± 0.15
	2.97 ± 0.08	Back cup	2.63 ± 0.04	2.14 ± 0.03	101.6 ± 1.4	13.96 ± 0.19

Uncertainty levels are given as the standard deviation of the mean with a 99.73 % confidence interval.

All the presented accumulated mass evaporation fluxes given in Figure 10 are calculated averages from a minimum of three measurement periods of 4 hours for Baumberger sandstone specimens and water surface at an air velocity of about 3.0 m/s.

As expected both for Baumberger and water surface it is observed that the evaporation mass per unit area is largest for the first upstream line. Thereafter follows the middle line. The lowest value of the mass evaporation per area is noted for the third downstream line, which in fact has the thickest velocity boundary layer thickness. Increasing the local position further away from the entrance of the wind tunnel increases the velocity boundary layer thickness, thus resulting in a decrease in the convective moisture transfer coefficient and accumulated evaporation fluxes (see Figure 1 for boundary layer development).

4.4 **Correlation between CMTC and diffusion resistance factor μ**

It should be noted that Baumberger sandstone has the largest porosity (0.23 m^3/m^3) of all the four stone materials, the three others having a porosity of 0.13 m^3/m^3 (Table 1). Furthermore it is seen (Table 1) that Baumberger sandstone has the lowest diffusion resistance factor μ (μ = 20), followed by Worzeldorfer sandstone (μ = 26), Sander sandstone (μ = 33) and Krensheimer shelly limestone (μ = 140). It is noted that Krensheimer shelly limestone has a substantially larger diffusion resistance factor μ than the three sandstones, which is also observed from the results in Figures 6-8 and Table 2.

A correlation between the convective moisture transfer coefficient (CMTC) (Table 2) and the diffusion resistance factor μ (Table 1) is depicted in Figure 11, indicating a linear relationship for three different air velocities within this material range. However, only four stone materials have been measured at three air velocities, so one should not draw too strong conclusions. Nevertheless, that there exists a correlation between the CMTC and the diffusion resistance factor μ seems evident, although other material properties and factors will probably also influence on these matters.

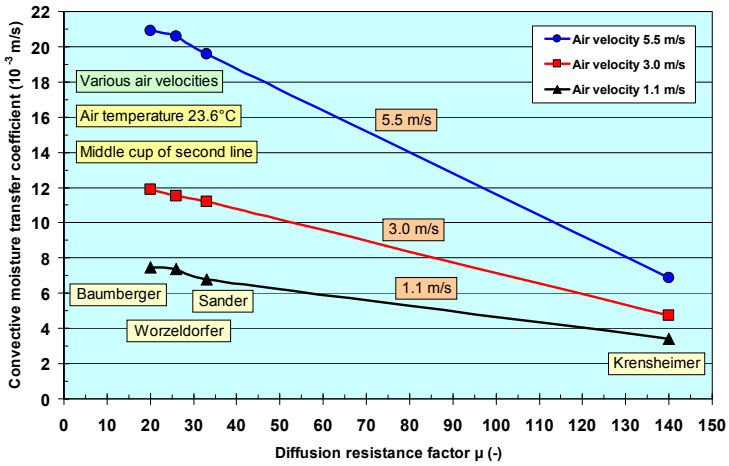

Figure 11. Convective moisture transfer coefficient vs. diffusion resistance factor μ for the four stone materials at three different air velocities.

5 CONCLUSIONS

The amount of water evaporated from several building materials, with their surfaces kept at a very high moisture content state, has been studied experimentally in a wind tunnel at three different wind velocities, three different air temperatures and three different local positions.

It was found that the experimental wind tunnel method was able to measure the convective moisture transfer coefficient and distinguish between various materials within acceptable uncertainty levels.

Based on the results from the wind tunnel experiments convective moisture transfer coefficients with corresponding uncertainties were calculated for six materials including the water reference, three air velocities, three air temperatures and three local positions in the wind tunnel. These results and calculations shows that (a) increasing the air velocity decreases the boundary layer thickness, hence leading to a higher convective moisture transfer coefficient, (b) increasing the air temperature increases the surface temperature difference between the ambient air temperature and the water film at the material surface, thus causing a higher convective moisture transfer coefficient, and (c) increasing the local position further away from the entrance in the wind tunnel increases the boundary layer thickness, hence leading to a lower convective moisture transfer coefficient. In addition, within this material range, the results indicate (d) a linear relationship between the convective moisture transfer coefficient and the diffusion resistance factor μ, although other material properties and factors will probably also influence on these aspects.

Studies ahead may include several other materials at different wind tunnel air velocities, air temperatures and relative air humidity levels, and may investigate the dependency of the

convective moisture transfer coefficient on surface roughness, material density, porosity, various evaporated areas and water absorption.

ACKNOWLEDGMENTS

The authors gratefully acknowledge Ole Aunrønning who provided practical support during various experimental work tasks.

REFERENCES

Carrier E.T. 1921. The theory of atmospheric evaporation with special reference to compartment dryers. *Journal of Ind. Eng. Chem.*, **13**, pp. 432-438.

Cengel A.Y. 2006. Heat and mass transfer a practical approach. 3rd ed., McGraw-Hill, USA, pp. 395-450.

Derome, D. 2004. Experimental determination of the convective mass transfer coefficient. Presented in IEA, ECBCS, Annex 41 Zurich, Switzerland.

Fraunhofer Institute. 2006. WUFI Pro, Version 4.2. Fraunhofer Institute, Stuttgart. Holzkirchen, Germany.

Grausse, P. Bacon G., and Langlais, C. 1985. Experimental and theoretical study of simultaneous heat and moisture transfer in a fibrous insulant. *Journal of Thermal Insulation*, **9**, pp. 46-67.

Hinchley, J.W., and Himus, G.W. 1924. Evaporation in currents air. *Trans. Inst. Chem. Eng.*, **2**, pp. 57-64.

Incropera F.P. and deWitt D.P. 2002. Fundamentals of heat and mass transfer. Third Edition, John Wiley and Sons, USA.

Iskra, C. and Simonson, C. 2005. Effect of air humidity on the convective mass transfer coefficient in a rectangular duct. Presented in IEA, ECBCS, Annex 41 Kyoto, Japan.

Jacobsen, S., and Aarseth, L.I. 1999. Effect of wind on drying from wet porous building materials surfaces – A simple model in steady state. *Journal of Materials and Structures*, **32**, pp. 38-44.

Jason A. C. 1958. A study of evaporation and diffusion processes in the drying of fish muscle, in fundamental aspects of dehydration of foodstuffs. *Soc. Chem. Ind.* (London) pp. 103-135.

Kays, W.M. and Crawford M.E. 1993. Convective heat and mass transfer. 3rd ed. Chap. 10. Heat transfer: The laminar external boundary layer. McGraw-Hill, USA, pp. 159-191.

Lurie, M., and Michailoff, N. 1936. Evaporation from free water surface. *Ind. Eng. Chem.*, **28**, pp. 345-349.

Talev, G., Gustavsen, A. and Næss, E. 2008(a). Influence of the velocity, local position, and relative humidity of moist air on the convective mass transfer coefficient in a rectangular tunnel – Theory and experiments. *Journal of Building Physics*, **32**, pp. 155-173.

Talev, G., Gustavsen, A. and Thue, J.V. 2008(b). Experimental confirmation on the theoretical model for velocity profile in a rectangular wind tunnel. *Proceedings of the 8th symposium on building physics in the Nordic countries.* (C. Rode, editor), Report R-189, Dept. of Civil Engineering, Technical University of Denmark. Kgs. Lyngby, Denmark pp. 331-338.

Talev, G., Jelle, B.P., Gustavsen, A., Thue J.V., and Aunrønning O. 2009. Measurement of convective mass transfer coefficients for building materials and air velocities in a wind tunnel. *Proceedings of the 4th international building physics conference: Energy Efficiency and New Approaches*. Bayazit, Maniglu, Oral and Yilmas (eds), Istanbul Technical University, ISBN 978-975-561-350-5, pp. 57-62.

Thomas W.C. 1977. Note on the heat transfer equation for forced convection flow over a flat plate with an unheated starting length. *Mechanical Engineering News*, **9**, no.1, pp. 361-368.

Wadsø L. 1993. Studies of water vapour transport and sorption in wood. *PhD thesis*, Building Materials, Lund University, Sweden, TVBM-1013 ISSN 0348-7911.

APPENDIX

Properties of the air and water surface that have been applied during the calculation procedure are given in Table A.

Table A. Material properties.

Air temp. (°C)	Water temp. (°C)	Air velocity (m/s)	Kinematic viscosity (10^6 m^2/s)	Sc (-)	φ (%)	Re (-)	P_s * (Pa)	P_∞ * (Pa)	ρ_s (kg/m^3)	ρ_∞ (kg/m^3)
23.60	20.08	1.1	15.7	0.62	50	15 765	2 339.0	1 318.9	1.19361	1.18363
23.60	20.04	3.0	15.7	0.62	50	42 994	2 342.3	1 318.9	1.19364	1.18363
23.60	20.00	5.5	15.7	0.62	50	78 822	2 345.6	1 318.9	1.19382	1.18363
26.50	22.70	3.0	15.8	0.61	50	42 994	2 936.6	1 468.3	1.18192	1.17149
30.00	25.90	3.0	16.0	0.60	50	42 994	2 828.7	1 584.5	1.16811	1.15744

* P_s and P_∞ are taken from Cengel (2006).